dicating that the diaphragm was not removed sufficiently at the time of flow arrival to avoid producing a disturbance at the nozzle entrance. That reasonably good quality pitot pressure time histories were measured for time intervals nearly equal to or somewhat less than the opening time is attributed to the close positioning of the nozzle entrance to the diaphragm. This permits the diaphragm to open cleanly to approximately the entrance diameter of 8.9 cm, instead of the tube diameter of 15.4 cm, to avoid significantly disturbing the nozzle-entrance flow. (Pitot pressure magnitudes, during the period of nearly constant pitot pressure, were within 10% of the mean value for no tertiary diaphragm and time intervals equal to 1160, 960, 760, and 560 μsec. This implies that nozzle flow started for no diaphragm and for time intervals less than the diaphragm opening time.)

The present tests demonstrated that a significant pressure lag effect exists for pitot pressure probes in which the pressure transducer is protected from particle contamination in the post-test flow by a perforated disk arrangement.[3] This effect is illustrated in Fig. 3, where pitot pressure time histories for a flush-mounted pressure transducer and a protected pressure transducer are shown for tests with no tertiary diaphragm and the self-opening diaphragm for $\Delta\tau \approx 1160$ μsec. The protective arrangement used in this study did not produce a pressure lag effect in expansion tube tests, where the pitot pressure was approximately 100 times that measured at the tunnel exit,[3] nor in calibration shock-tube tests for pitot pressures as low as 8 to 10 kN/m^2. Also, the preliminary expansion tunnel pitot pressure measurements presented in Ref. 3, which did not employ a tertiary diaphragm, gave no indication of the existence of a pressure lag effect as demonstrated in Fig. 3. However, by reducing the magnitude of the starting nozzle shock, the self-opening diaphragm data reveal that erroneous conclusions may be drawn from pitot pressure time histories if the protector arrangement is used. For example, the present protector arrangement and quasisteady pitot pressure magnitude of about 2.5 kN/m^2 yields a pressure lag time roughly 300 to 400 μsec, or nearly equal to the quasisteady flow duration.

References

[1] Weilmuenster, K. J., "A Finite-Difference Analysis of the Nozzle Starting Process in an Expansion Tunnel," NASA TN D-8105, 1975.

[2] Moore, J. A., "Measured Opening Characteristics of an Electromagnetically Opened Diaphragm for the Langley Expansion Tunnel," NASA TM X-3378, 1976.

[3] Miller, C. G., "Operational Experience in the Langley Expansion Tube with Various Test Gases and Preliminary Results in the Expansion Tunnel," AIAA Ninth Aerodynamic Testing Conference, June 7-9, 1976.

[4] Moore, J. A., "Description and Initial Operating Performance of the Langley 6-Inch Expansion Tube Using Heated Helium Driver Gas," NASA TM X-3240, 1975.

Response of Cantilever Columns under Transient Follower Forces

S. T. Nouh* and V. Sundararajan*
Pontificia Universidade Catolica, Rio de Janeiro, Brazil

Introduction

THERE has been an increasing interest in the problem of dynamic stability of columns subjected to transient axial loads. Holzer and Eubanks[1] and Holzer,[2] employing Liapunov's method, explicitly obtained a bound on the transverse motion of elastic columns subjected to a transient compressive force. McIvor and Bernard[3] studied the dynamic response of a simply supported column subjected to short duration axial loads including the effects of axial inertia. These works consider the transient loads to act axially. The present paper deals with the elastic response of a cantilever column to a transient compressive follower load. Material dissipation is included by means of a Kelvin model for the material behavior. The amplification of the lateral response of the column is obtained assuming a set of initial perturbations. The effect of pulse duration, internal damping, and different initial perturbations are investigated. The present study is applicable to the analysis of the response of a severed pipeline conveying fluids under high pressure. The objective would be, to determine whether the pipe deforms enough to damage adjacent equipment and structure

Received Feb. 2, 1977; revision received April 12, 1977.
Index categories: Structural Dynamics; Structural Stability.
*Departamento Engenharia Mecânica.

Formulation and Solution

The equation of motion for the small lateral vibration of a column of length ℓ and flexural rigidity EI loaded axially by a follower force $P_0(\tau)$ can be written in nondimensional form as

$$\frac{\partial^4 w}{\partial \xi^4} + \gamma \frac{\partial^5 w}{\partial \xi^4 \partial \tau} + P(\tau) \frac{\partial^2 w}{\partial \xi^2} + \frac{\partial^2 w}{\partial \tau^2} = 0 \qquad (1)$$

where

w = transverse deflection

$\gamma = \frac{\mu}{\ell^2}\left[\frac{I}{Em}\right]^{1/2}$ = dimensionless dissipation parameter

μ = internal damping coefficient

$\tau = \left[\frac{EI}{m}\right]^{1/2} \frac{t}{\ell^2}$ = dimensionless time

m = mass per unit length

$P(\tau) = \frac{P_0(\tau)\ell^2}{EI} \geq 0$ in $(0,\tau)$ and $P(\tau) = 0$ when $\tau > \tau^*$.

Assumption of a solution in the form

$$w(\xi,\tau) = \Sigma Y_n(\xi) q_n(\tau) \qquad n = 1,2,\ldots \qquad (2)$$

where $Y_n(\xi)$ are the normal modes of the freely vibrating column, and application of Galerkin's techique leads to

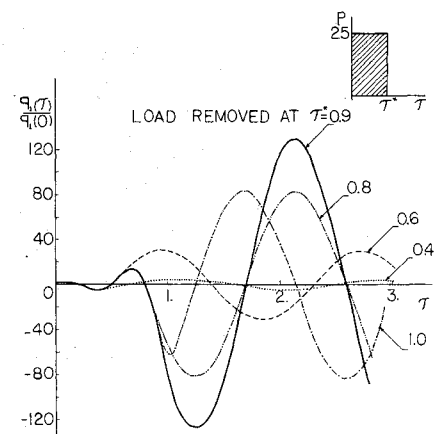

Fig. 1 Variation of q_1 with τ for various pulse duration τ^*.

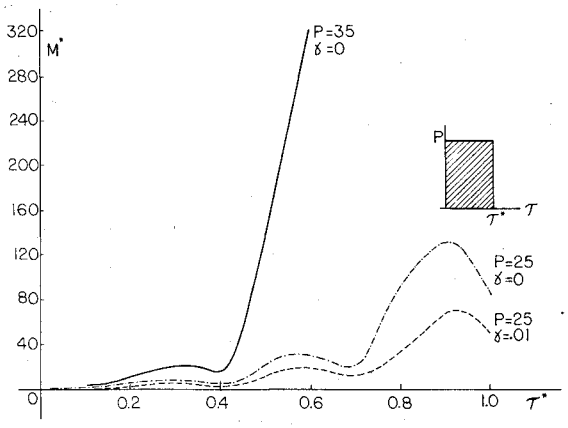

Fig. 2 Maximum magnification factor vs the pulse duration.

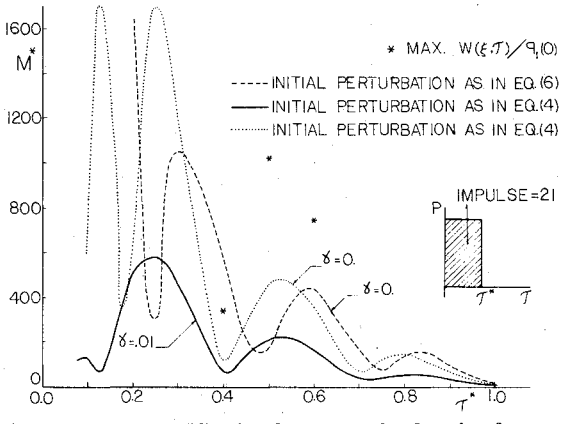

Fig. 3 Maximum magnification factor vs pulse duration for constant impulse rectangular pulse.

reduction of Eq. (1) to

$$\ddot{q}_m + \gamma\beta_m^4 \dot{q}_m + \beta_m^4 q_m + P(\tau)\sum_n q_n \phi_{mn} = 0 \quad m = 1,2,\ldots \tag{3}$$

where β_m are the roots of the frequency equation for the free undamped vibration of the column and $\phi_{mn} = \int_0^1 Y_m(\xi)\, Y_n''(\xi)\, d\xi$. A dot and a prime indicate differentiation with respect to τ and ξ respectively.

The coupled equations (3) were integrated numerically. Convergence of the solution was tested by increasing m and observing the asymptotic nature of the solution. The final computation was done using six terms.

Results and Discussion

The numerical solution of Eq. (3) is performed for the following cases: 1) rectangular pulse with amplitude $P=25$ and 35 and different pulse durations τ^*, and 2) rectangular pulse with constant impulse of 21. Initial conditions of the following form were assumed:

$$q_1(0) = 10^{-4}; \qquad q_m(0) = 0, \qquad m > 1 \tag{4}$$

Figure 1 shows the relation of $q_1(\tau)/q_1(0)$ with τ for various values of the duration τ^* of the rectangular pulse with $P=25$. Since the response is dominated by the first mode, only $q_1(\tau)$ is shown. It can be seen that the maximum amplification of the initial disturbance depends on the time at which the load is released and always occurs after the release of the load. As a measure of the total response, the magnification factor

$$M = [\Sigma q_m^2(\tau)]^{1/2} / [\Sigma q_m^2(0)]^{1/2} \tag{5}$$

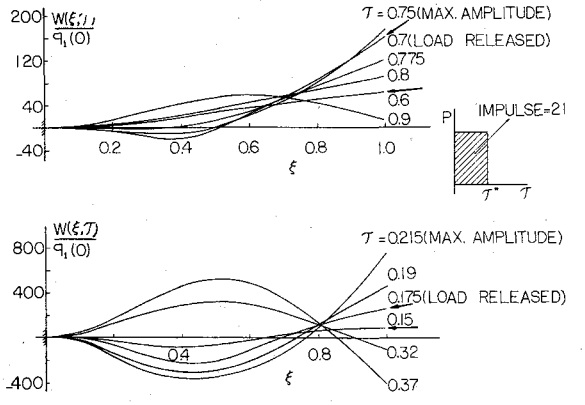

Fig. 4 Response history of the column.

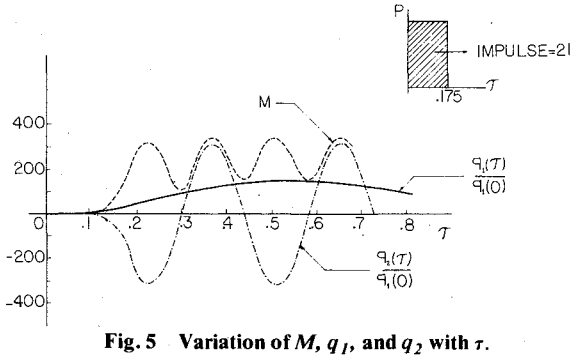

Fig. 5 Variation of M, q_1, and q_2 with τ.

is introduced. The variation of the maximum M^* of the magnification factor with τ^* is shown in Fig. (2). M^* becomes very large when τ^* is sufficiently large, indicating that the column experiences a flutter instability. Also shown in the figure is the effect of internal damping.

Results corresponding to a rectangular pulse with constant impulse are displayed in Figs. 3 to 5. The initial perturbations are of the form given in Eq. (4). The effect of the pulse duration τ^* on the maximum magnification M^* is shown in Fig. 3. M^* depends on the pulse duration, the strain energy of the beam at the time the load is released, and the work done by the nonconservative part of the applied tangential load. Also shown in Fig. 3 is the effect of internal damping. For small τ^* the effect of internal damping is considerable and for values of τ^* approximately unity and above, M^* is more than the value corresponding to no damping. The latter is due to the well known fact that a small amount of damping decreases the critical load in the case of tangential forces. The actual history of the response $w(\xi,\tau)$ of the beam column corresponding to $\tau^* = 0.175$ and 0.7 are shown in Figs. 4a and 4b. As can be expected the maximum deflection occurs at the free end of the column, It is of interest to compare the maximum deflection at the end with that predicted with use of the maximum magnification factor. Even though use of the maximum magnification factor yields the same trend as that of the actual amplification, the latter amplitude is about twice the former. The maximum amplification, max $[w(\xi,\tau)/q_1(0)]$, has been denoted by an asterisk mark in Fig. 3. The variation of M^* with τ^* is plotted in Fig. 3 for a different initial perturbation of the form

$$q_m(0) = 10^{-4}/m^2 \tag{6}$$

It can be noticed that this type of initial perturbation has a large influence on the maximum magnification factor, particularly when the pulse duration is small.

Figure 5 shows an interesting case in which the second mode dominates the overall response even though the initial perturbation is assumed to contain the first mode only, Eq. (4).

This case corresponds to $\tau^* = 0.175$ and an impulse of 21. The actual response history of the beam is shown in Fig. 4b.

References

[1] Holzer, S.M. and Eubanks, R.A., "Stability of Columns Subjected to Impulsive Loading," *Proceedings of the American Society of Civil Engineers; Journal of the Engineering Mechanics Division,* Vol. 95, No. EM4, 1969.

[2] Holzer, S.M., "Response Bounds for Columns With Transient Loads," *Journal of Applied Mechanics,* Vol. 38, No. 1; *Transactions of the ASME, Series E,* Vol. 93, March 1971, pp. 157-161.

[3] McIvor, I.K. and Bernard, J.E., "The Dynamic Response of Columns under Short Duration Axial Loads," *Journal of Applied Mechanics,* Vol. 40, No. 3; *Transactions of the ASME,* Series E, Vol. 95, Sept. 1973, pp. 688-692.

An Estimate of Mean Flow Properties in a Turbulent Diffusion Flame

Louis H. Bangert*
Georgia Institute of Technology, Atlanta, Ga.

Introduction

SOME recent models for the computation of turbulent diffusion flames have included effects of fluctuations of concentration and temperature on the flow behavior.[1-6] These theories have neglected some second-order correlations involving density fluctuations, however, so that the level of modeling may not be completely consistent. For shear flows composed of species of widely differing molecular weights, density fluctuations may be large,[7] and some correlations involving them may not be negligible.[8]

This study considered a simpler approach, in which turbulent diffusion flames were computed while neglecting fluctuations of density, concentration, or temperature. An estimate for the time-average rate of consumption of the fuel specie $\bar{w}_f(\sec^{-1})$ was made, based mainly on dimensional analysis. First, it was assumed that mixing of the reactants is the rate-controlling step. This process occurs on the macroscale of the turbulence.[7] For a turbulent velocity scale, $k^{0.5}$, and a turbulent length scale, $k^{1.5}/\epsilon$, $\bar{w}_f$ can be assumed to be proportional to ϵ/k. Here k is the turbulent kinetic energy per unit mass, and ϵ is the rate of dissipation of turbulent energy per unit mass. This is essentially the form proposed by Spalding[9] for premixed turbulent flames. It also was assumed that $\bar{w}_f$ is a function of $\bar{C}_f$ and $\bar{C}_o$, the time-average mass fractions of fuel and oxidizer, respectively. In order that $\bar{w}_f$ goes to zero when either reactant disappears, a general form $\bar{w}_f = -A(\epsilon/k)\,\bar{C}_f^m \bar{C}_o^n$ was assumed, where A, m, and n are positive constants. Having three constants would seem to provide wide latitude in curve fitting a given set of experimental data. However, the results of computations suggest that the simple choice $m = n = 1$, with A determined empirically, may be adequate to represent the data.

Results

Calculations were made for the experimental conditions of Kent and Bilger.[10] The experimental arrangement was a central hydrogen jet issuing into a parallel, coaxial airstream. The initial and boundary conditions for the calculations were the same as those measured. Initial values for k were determined from the measured $\overline{u'^2}$ by $k \cong \overline{u'^2}/4\,C_\mu^{0.5}$, where $C_\mu \cong 0.09$ (Ref. 11). Initial values of ϵ were determined from $\epsilon \cong C_\mu^{0.5} k\,\partial\bar{U}/2r$.

Received Jan. 19, 1977; revision received April 6, 1977.
Index categories: Airbreathing Propulsion; Combustion and Combustor Designs.

*Associate Professor, School of Aerospace Engineering. Member AIAA.

The flowfield solution used the time-averaged conservation equations for mass, momentum, energy, species mass fraction, k, and ϵ for axisymmetric flow in the boundary-layer approximation. Various correlations were modeled as described by Launder and Spalding.[12] Values of the empirical constants in the k and ϵ equations were also the same as those given in Ref. 12. A mixture of perfect gases with variable specific heats was assumed.

Results for two forms of the equation for $\bar{w}_f$ are given in what follows. The first and simplest form is

$$\bar{w}_f = -A(\epsilon/k)\,\bar{C}_f \bar{C}_o \tag{1}$$

Using the experimental data of Kent and Bilger[10] for the case where $\bar{U}_j/\bar{U}_e = 10$, the value $A = 12$ was found to give the best agreement with the measured centerline variations of temperature and of the mole fractions of H_2, H_2O, and O_2. These results are shown in Fig. 1. Here, $\bar{U}_j$ is the jet mass-average velocity and $\bar{U}_e$ is the mean freestream velocity. These results seemed to be relatively insensitive to the value of A, as variations of up to about 30% had only small effects on the computed flow properties.

Calculations also were made for the following form:

$$\bar{w}_f = -B(\epsilon/k)\,\bar{C}_f \bar{C}_o^{0.5} \tag{2}$$

Again, using the centerline experimental data for $\bar{U}_j/\bar{U}_e = 10$, the value $B = 4$ gave the best agreement. These results also are shown in Fig. 1 and differ only slightly from those obtained using Eq. (1). Figure 1 also shows computed distributions of

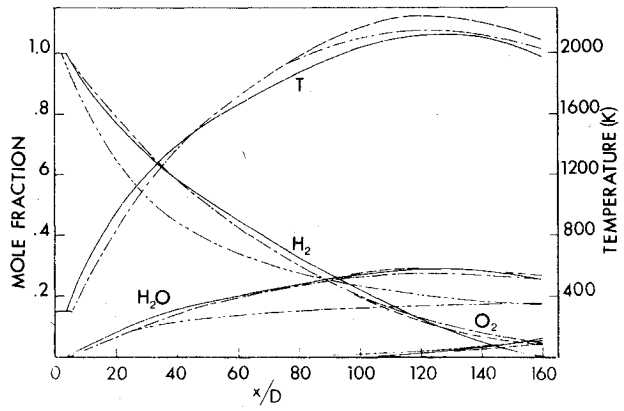

Fig. 1 Centerline values of temperature and mole fractions for $\bar{U}_j/\bar{U}_e = 10$. —— experiment,[10] –·– calculation using (1), - - - calculation using (2), – – – calculation with no reaction.

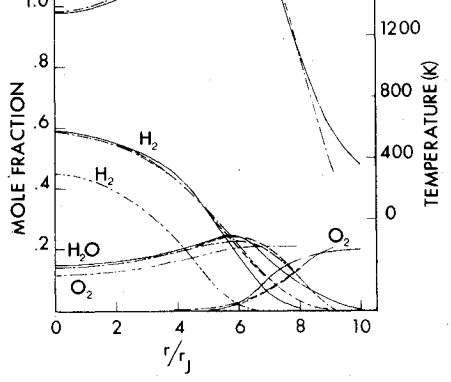

Fig. 2 Radial variation of temperature and mole fractions at $x/D = 40$ for $\bar{U}_j/\bar{U}_e = 10$. —— experiment,[10] legend as in Fig. 1.